Projected Changes in Mean and Extreme Precipitation over Northern Mexico

ROBERT H. NAZARIAN,[a] NOEL G. BRIZUELA,[b] BRODY J. MATIJEVIC,[a] JAMES V. VIZZARD,[a] CARISSA P. AGOSTINO,[a] AND NICHOLAS J. LUTSKO[b]

[a] *Department of Physics, Fairfield University, Fairfield, Connecticut*
[b] *Scripps Institution of Oceanography, University of California at San Diego, La Jolla, California*

(Manuscript received 26 June 2023, in final form 18 January 2024, accepted 22 January 2024)

ABSTRACT: Northern Mexico is home to more than 32 million people and is of significant agricultural and economic importance for the country. The region includes three distinct hydroclimatic regions, all of which regularly experience severe dryness and flooding and are highly susceptible to future changes in precipitation. To date, little work has been done to characterize future trends in either mean or extreme precipitation over northern Mexico. To fill this gap, we investigate projected precipitation trends over the region in the NA-CORDEX ensemble of dynamically downscaled simulations. We first verify that these simulations accurately reproduce observed precipitation over northern Mexico, as derived from the Multi-Source Weighted-Ensemble Precipitation (MSWEP) product, demonstrating that the NA-CORDEX ensemble is appropriate for studying precipitation trends over the region. By the end of the century, simulations forced with a high-emissions scenario project that both mean and extreme precipitation will decrease to the west and increase to the east of the Sierra Madre highlands, decreasing the zonal gradient in precipitation. We also find that the North American monsoon, which is responsible for a substantial fraction of the precipitation over the region, is likely to start later and last approximately three weeks longer. The frequency of extreme precipitation events is expected to double throughout the region, exacerbating the flood risk for vulnerable communities in northern Mexico. Collectively, these results suggest that the extreme precipitation-related dangers that the region faces, such as flooding, will increase significantly by the end of the century, with implications for the agricultural sector, economy, and infrastructure.

SIGNIFICANCE STATEMENT: Northern Mexico regularly experiences severe flooding and its important agricultural sector can be heavily impacted by variations in precipitation. Using high-resolution climate model simulations that have been tested against observations, we find that these hydroclimate extremes are likely to be exacerbated in a warming climate; the dry (wet) season is projected to receive significantly less (more) precipitation (approximately ±10% by the end of the century). Simulations suggest that some of the changes in precipitation over the region can be related to the North American monsoon, with the monsoon starting later in the year and lasting several weeks longer. Our results also suggest that the frequency of extreme precipitation will increase, although this increase is smaller than that projected for other regions, with the strongest storms becoming 20% more frequent per degree of warming. These results suggest that this region may experience significant changes to its hydroclimate through the end of the century that will require significant resilience planning.

KEYWORDS: Extreme events; Monsoons; Precipitation; Hydrology; Regional models

1. Introduction

Changes in precipitation resulting from anthropogenic global warming are already putting significant stress on human activities, and simulations of future climate scenarios project that the burden of extreme weather and precipitation events is likely to worsen over the coming decades (Donat et al. 2016; Tabari 2020). Adapting to these changes will be a major challenge for a wide variety of stakeholders, and requires detailed and reliable projections of future precipitation. A growing number of studies have sought to provide such projections, primarily focusing on the United States and Europe, where most climate research is carried out (Rajczak et al. 2013; Lopez-Cantu et al. 2020; Nazarian et al. 2022). Unfortunately, this has left large gaps, especially in the Global South, where some of the world's most vulnerable populations reside. Filling out our projections of future changes in precipitation to include regions outside those traditionally studied is important to ensure these areas have access to climate information in order to adapt to potential future changes.

Observations and reanalysis products suggest that precipitation has increased over northwestern Mexico (Gutiérrez-Ruacho et al. 2010), with some studies tying the increase in precipitation to the North American monsoon (Diem et al. 2012; Lahmers et al. 2016; Pascale et al. 2019). Similarly, simulations over the historical period have likewise captured the increase in extreme precipitation over northwestern Mexico due to the North American monsoon (Luong et al. 2017). Furthermore, observations have suggested that summertime extreme precipitation has increased in both northwestern and northeastern Mexico due to tropical cyclones (Colorado-Ruiz and Cavazos 2021). Simulations of future climate scenarios indicate that the burden of extreme weather and precipitation

Denotes content that is immediately available upon publication as open access.

Corresponding author: Robert H. Nazarian, rnazarian@fairfield.edu

DOI: 10.1175/JCLI-D-23-0390.1

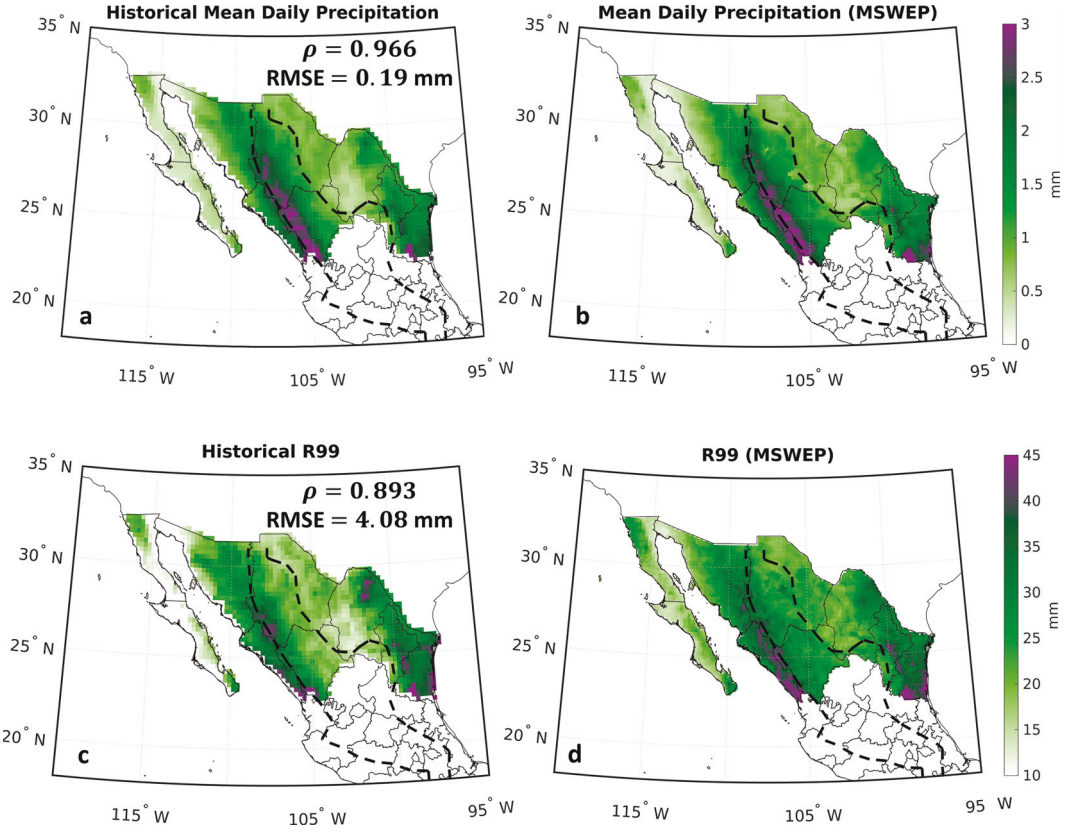

FIG. 1. Comparison between (a),(b) mean and (c),(d) R99 daily precipitation in historical (a),(c) NA-CORDEX simulations and (b),(d) MSWEP data. The correlation coefficients ρ and root-mean-square error (RMSE) quantify the agreement between model output and observations. The black dashed line denotes the Sierra Madre highlands. We define the historical period as 1986–2005.

events is likely to worsen over the coming decades (Caparas et al. 2021). Several modeling studies utilizing a high-emissions scenario suggest changes in the North American monsoon by the end of the twenty-first century, with some suggesting a drier monsoon (Pascale et al. 2017; Colorado-Ruiz et al. 2018; He et al. 2020; Ashfaq et al. 2021), thus reducing seasonal precipitation over vast areas of central and northwestern Mexico (Almazroui et al. 2021), while others project a delayed monsoon (Cook and Seager 2013; Meyer and Jin 2017). However, there is uncertainty about the sign of precipitation changes in other regions of Northern Mexico (Caparas et al. 2021; Almazroui et al. 2021) and evidence suggesting future shifts in the seasonality of the North American monsoon (Ashfaq et al. 2021) warrant further study of projected precipitation scenarios.

In this study, we take advantage of an ensemble of high-resolution climate simulations originally designed to study climate change over the United States, and use it to provide detailed projections of changes in mean and extreme precipitation over northern Mexico (see territorial definition in Fig. 1), which is home to 32 million people and includes numerous areas with high risk of and and vulnerability to drought, heatwaves, and flooding (Ortega-Gaucin and Velasco 2013; Díaz Caravantes et al. 2014; Aguilar-Barajas et al. 2019). The region accounts for 27% of Mexico's gross area dedicated to agriculture and 32% of its agricultural revenue (INEGI 2020), and without proper adaptation, substantial precipitation changes as a result of future warming could lead to major social and economic disruptions (Magaña et al. 2021). Policies for climate adaptation in this region must account for possible changes in mean and extreme precipitation patterns over the coming decades, and while some studies have been important in providing some projections for future trends in the hydroclimate of northern Mexico (Cavazos and Arriaga-Ramírez 2012; Seager et al. 2013; Torres-Alavez et al. 2014; Colorado-Ruiz et al. 2018), significant questions remain.

To study future trends in mean and extreme precipitation over the region, we use the Coordinated Regional Climate Downscaling Experiment (CORDEX) ensemble, which consists of dynamically downscaled global climate model (GCM) simulations, derived from the latest Climate Model Intercomparison Project (CMIP5) ensemble (Giorgi and Gutowski 2015). Earlier studies have illustrated the "added value" that dynamically downscaling GCM simulations using high-resolution regional climate models (RCMs) provides by capturing smaller-scale processes as compared to using GCMs alone (Diffenbaugh et al. 2005; Di Luca et al. 2012; Ashfaq et al. 2016; Lucas-Picher et al. 2017). Of particular relevance here, RCMs better capture the mesoscale phenomena, such as mesoscale convective systems (MCS) or monsoonal moisture surges, that lead to extreme precipitation.

TABLE 1. Global and regional model pairings of the 12 NA-CORDEX simulations with daily output that have been bias-corrected using the Daymet observational dataset. All model pairings considered here have 0.22° (~25-km) resolution and are forced with the RCP8.5 scenario. The equilibrium climate sensitivity (ECS; the temperature increase due to a doubling of CO_2), was previously diagnosed by the NA-CORDEX team (see https://na-cordex.org/simulation-matrix.html) and is provided here for each model.

Global model	Regional model	ECS (°C)
CanESM2	CanRCM4	3.7
	CRCM5-UQAM	3.7
GEMatm-Can	CRCM5-UQAM	3.7
GEMatm-MPI	CRCM5-UQAM	3.6
GFDL-ESM2M	RegCM4	2.4
	WRF	2.4
HadGEM2-ES	RegCM4	4.6
	WRF	4.6
MPI-ESM-LR	CRCM5-UQAM	3.6
	RegCM4	3.6
	WRF	3.6
MPI-ESM-MR	CRCM5-UQAM	3.4

Furthermore, RCMs provide better representation of orography, (Leung et al. 2003), which is critically important in setting up the hydroclimate of northern Mexico, and better capture the atmosphere's regional-scale circulation, both of which contribute to more realistic projections of extreme precipitation. We note, however, that neither GCMs nor RCMs are able to accurately simulate convectively driven extreme precipitation (O'Gorman 2015; Prein et al. 2017; Muller and Takayabu 2020).

We focus specifically on the NA-CORDEX ensemble, which provides downscaled simulations over the North American region (with approximate longitudinal bounds of 62°–169°W and latitudinal bounds of 19°–68°N), including northern Mexico. NA-CORDEX has been used to investigate future climate change over the United States (Bukovsky and Mearns 2020; Lopez-Cantu et al. 2020; Nazarian et al. 2022), but to our knowledge has not previously been used to study climate change over Mexico specifically. Other studies using CORDEX-CAM, which covers Central America, the Caribbean, and Mexico, have been used to analyze changes in precipitation over Mexico (Cavazos et al. 2019; Luna-Niño et al. 2021), although they have not exclusively focused on the northern region as we do here. The NA-CORDEX domain does not extend over the entire country of Mexico, but does include a significant portion of the country, including the entirety of northern Mexico. Precipitation climatology over northern Mexico is be characterized by high precipitation on the Gulf of California and Gulf of Mexico–facing slopes of the Sierra Madre highlands where moist upslope flow occurs, with the highest levels of precipitation occurring in the Gulf of California side due to the North American monsoon during mid- to late summer (Hastings and Turner 1965; Adams and Comrie 1997; Cavazos 1997; Mendoza et al. 2005; Gochis et al. 2006; Stahle et al. 2009). Furthermore, the eastern side of the Sierra Madre highlands experiences peaks in summer and fall precipitation driven by convective systems, easterly waves, and tropical cyclones (Breña Naranjo et al. 2015; Colorado-Ruiz et al. 2018), as well as easterly moisture transport from the Gulf of Mexico (Jáuregui 2003).

We begin by assessing the ability of the NA-CORDEX to simulate present-day precipitation over northern Mexico by comparing historical simulations with observations derived from the Multi-Source Weighted-Ensemble Precipitation (MSWEP) product in section 3. After demonstrating that NA-CORDEX accurately reproduces observed rainfall statistics, we quantify future trends in mean and extreme precipitation over the region in sections 4a and 4b, respectively. Given the role of the North American monsoon on the seasonality of extreme precipitation over northern Mexico, we investigate changes in the characteristics of the monsoon in section 4c, including its onset timing and length. In section 4d, we focus on five cities, representing different regions of northern Mexico, as case studies for future trends in extreme precipitation. We provide a synthesis of results and discuss implications in section 5.

2. Methods

a. *The NA-CORDEX ensemble*

To diagnose future changes in precipitation over northern Mexico, we use the dynamically downscaled NA-CORDEX ensemble. CORDEX downscales a suite of GCMs from CMIP5 using a number of RCMs (see Table 1 for a list of the GCM and RCM pairings). CORDEX is ideal for studying regional changes in hydroclimate and has been employed in numerous studies of other regions (Lopez-Cantu et al. 2020; Rendfrey et al. 2021; Nazarian et al. 2022).

We use the NA-CORDEX simulations run at 0.22° (~25-km) horizontal resolution, as previous studies have shown that higher-resolution models provide more accurate estimates of precipitation (Lucas-Picher et al. 2017) [see the data availability statement for instructions for accessing the NA-CORDEX data and Bukovsky and Mearns (2020) for a description of NA-CORDEX]. The only set of NA-CORDEX simulations conducted at higher resolution were forced with reanalysis data, and so cannot be used to make climate projections. A 0.22° resolution is sufficiently high to capture hydroclimate variations over northern Mexico, which we define to include the states of Baja California, Baja California Sur, Sonora, Chihuahua, Durango, Sinaloa, Nuevo León, Tamaulipas, and Coahuila (see Fig. 1 for an illustration of this region). All variables are taken at the surface; data at higher atmospheric levels are not publicly available. We use data that have been bias-corrected using the daily Daymet observational dataset, which is accepted practice for studying climate impacts (Kirchmeier-Young et al. 2017; Cannon 2018; McGinnis and Mearns 2021; Nazarian et al. 2022). Notably, the Daymet bias-correction process does not remove all bias, and there are still differences in the model climatologies.

While the NA-CORDEX simulations span 1950–2100, we focus on two 20-yr periods. We take the "historical" period to be 1986–2005, the "projected" period to be 2081–2100, and report changes as the difference between the two (i.e., projected minus historical). Unless otherwise stated, we use daily-averaged values for all variables. The simulations are forced with the RCP8.5 emission scenario (i.e., a "high-emissions" scenario) for the period 2006–2100. While it is too soon to know which emissions pathway we will follow through the end of the century, we utilize

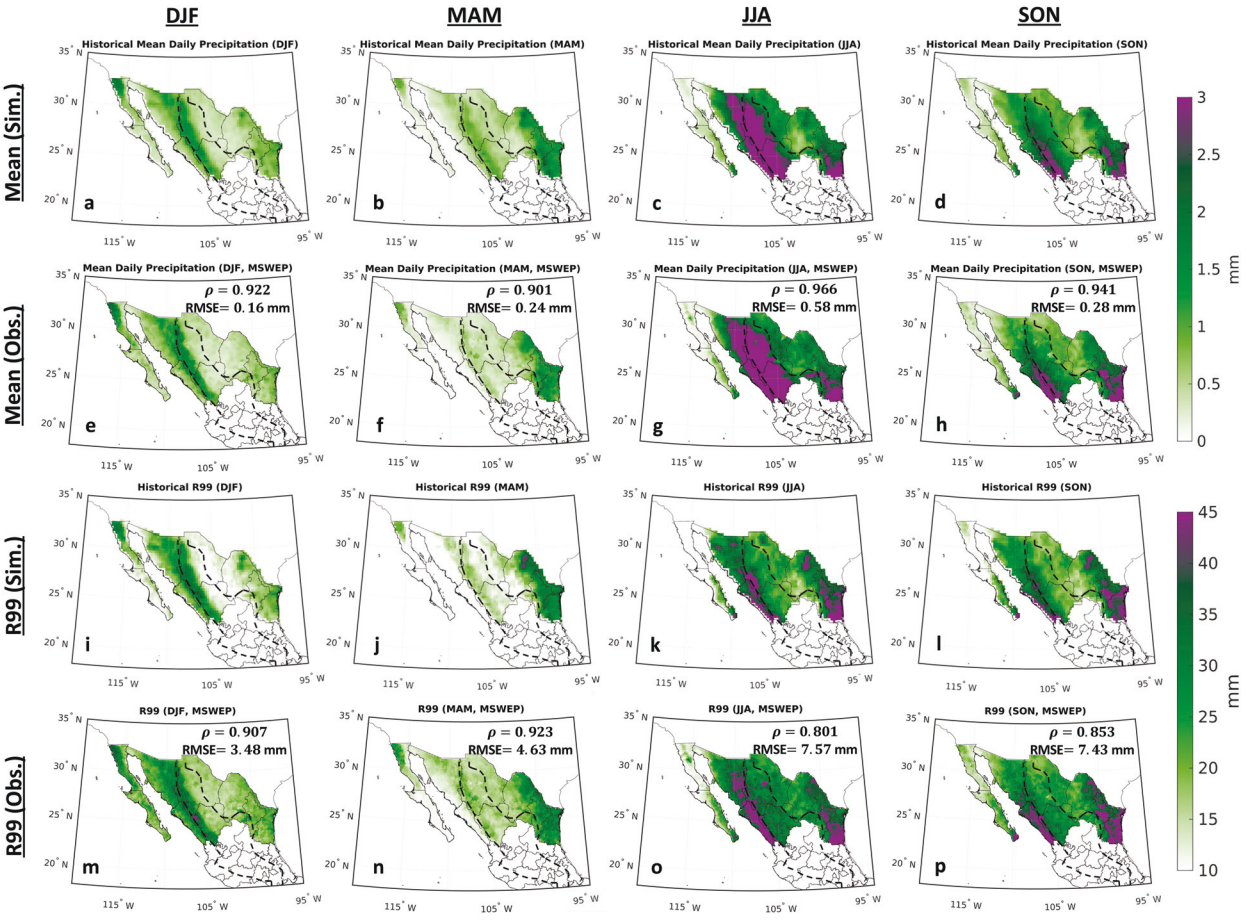

FIG. 2. Comparison between seasonal (a)–(h) mean and (i)–(p) R99 daily precipitation in historical NA-CORDEX simulations and MSWEP data. The correlation coefficients (ρ) and root-mean-square error (RMSE) in (e)–(h) and (m)–(p) quantify the agreement between model output and observations. As in Fig. 1, the black dashed line denotes the Sierra Madre highlands.

RCP8.5 since there are more NA-CORDEX simulations conducted using this emissions scenario than there are for the other emissions scenarios. Pendergrass et al. (2015) showed that the fractional change in extreme precipitation (the percent change per degree of warming) is generally independent of the emissions scenario, so we do not expect that our use of RCP8.5 has a significant impact on our findings. In total, data from 12 simulations are available (Table 1), but we exclude one model pairing (CanESM2, CRCM2-UQAM) that produces an exceptionally large drying over the entire region. Investigating why this pairing produces such outlier behavior is a topic of future work.

Even with one simulation excluded, the range of equilibrium climate sensitivities across the simulations is 2.4°–4.6°C, which provides nearly the same range in climate sensitivity as the full CMIP5 ensemble [2.0°–4.7°C] (Andrews et al. 2012; Flato et al. 2013). Additionally, the spread in projections of annual-mean North American precipitation from the dynamically downscaled NA-CORDEX simulations is greater than that of the driving GCMs, and close to that of the full CMIP5 ensemble (Bukovsky and Mearns 2020). Regardless of the global or regional model used, however, all simulations slightly underestimate the magnitude of average annual, accumulated precipitation over northern Mexico [approximately 0.473 m, as calculated from the MSWEP (see description of this observational product in the next section)].

b. *MSWEP*

MSWEP (version 2.8) is a global precipitation product that uses a combination of gauge-, satellite-, and reanalysis-based data (Beck et al. 2017, 2019). The MSWEP dataset begins in 1979 and continues through the present. MSWEP is ideal for studying regional hydroclimate given both its high spatial (0.1°) and temporal (3-h) resolution and, as such, has been used in a number of earlier studies (Sharifi et al. 2019; Xu et al. 2019; Li et al. 2022). Furthermore, it is the only product to use a combination of gauges, satellites, and reanalyses to derive precipitation observations, which has been shown to particularly enhance its performance over convective- and frontal-dominated weather regimes (Beck et al. 2017). Additionally, the MSWEP data use an algorithm to account for gauge reporting times, which minimizes the mismatch between gauge observations and satellite/reanalysis estimates. We refer the reader to Beck et al. (2019) for more information about the data.

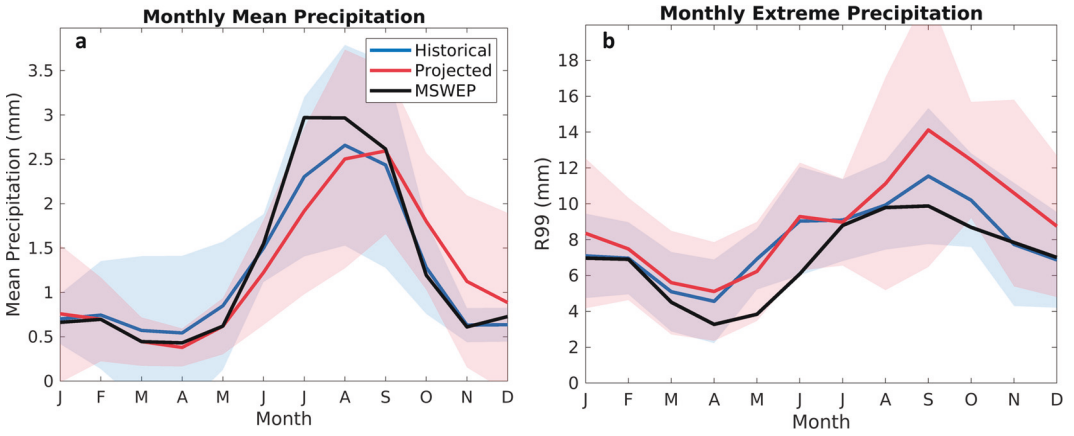

FIG. 3. Seasonal evolution of (a) mean daily and (b) R99 precipitation over all of northern Mexico in MSWEP data (black), historical (blue), and end-of-century (red) simulations. Solid lines indicate the multimodel means, while shading represents the 90% confidence intervals.

Like the NA-CORDEX historical output, we take the MSWEP data from 1986 to 2005. MSWEP and NA-CORDEX have different resolutions (0.10° vs 0.22°, respectively), so we regrid MSWEP to a 0.22° grid to conduct all calculations. We evaluate the skill of the NA-CORDEX ensemble by calculating the correlation coefficients between the NA-CORDEX ensemble average and the average of MSWEP observations. We do not detrend the MSWEP observations nor NA-CORDEX simulations to perform this comparison since we are conducting this comparison over the historical period.

c. *North American monsoon timing metrics*

The North American Monsoon (NAM) is responsible for providing approximately 70% of the annual precipitation over portions of northwestern Mexico (Reyes et al. 1994; Ramos-Pérez et al. 2022). While the dynamics governing the NAM are unique from other monsoons (notably the Indian monsoon), it is nevertheless characterized as a monsoon by its confinement to the summer months and its reversal of the surface winds (Barlow et al. 1998; Boos and Pascale 2021).

To study the projected changes in the NAM we define the NAM region to include the states of Baja California Sur, Sonora, Sinaloa, Chihuahua, and Durango, although we note that the precipitation each of these states experiences due to the monsoon may vary significantly. To calculate the timing of the NAM, we utilize the metric of Zhang et al. (2002), which defines the start of the monsoon as the first day on which a 5-day running-mean rainfall index exceeds 2 mm [this value is modified from the original Zhang et al. (2002) metric given the amplitude of the NAM relative to other monsoons] and persists continuously for 5 days. The monsoon state is defined as the period over which at least 10 out of every 20 days receive more than 2 mm of precipitation, with the end of the monsoon defined as when this criterion is no longer satisfied. We note that this metric is similar to that of Geil et al. (2013), although we use a slightly larger threshold value (2 mm compared to their 1.3 mm) due to the NA-CORDEX climatology. For each simulation, as well as for the MSWEP record, the monsoon start and end dates are calculated each year before any averaging is conducted.

d. *Extreme precipitation metrics*

While a number of metrics for extreme precipitation are used in the hydroclimate literature, such as the annual maximum daily precipitation, the number of a days in a year with precipitation exceeding 10 mm, and the threshold of the 99th percentile of precipitation (R99) (Nazarian et al. 2022), we use the R99 metric throughout our analysis, as it is of most use to planners and water managers. We calculate extreme precipitation statistics (Ban et al. 2015; O'Gorman 2015) using all days, rather than only wet days, since earlier studies have shown that the frequency of wet days is not constant in a warming climate (Schär et al. 2016).

Furthermore, we perform a similar frequency analysis as in Martinez-Villalobos and Neelin (2019) by considering daily, regionally averaged (weighted by area) mean and extreme precipitation for each simulation. Values are then averaged across the 11 simulations to derive the ensemble average. As in Nazarian et al. (2022), we calculate fractional changes in extreme precipitation using the local rate of warming rather than the global rate of warming. Specifically, we use local warming in order to provide regional stakeholders with a localized metric for planning. Additionally, we argue that the local change in temperature is more useful for diagnosing the drivers of changes in extreme precipitation at the spatial scales considered here.

3. Model assessment

There are two prominent wet areas in northern Mexico: one on the western side of the Sierra Madre highlands that is influenced by the NAM (Adams and Comrie 1997; He et al. 2020) and another along the eastern side for which late summer precipitation is governed by tropical cyclones and moisture fluxes from the Gulf of Mexico (Jáuregui 2003) and for

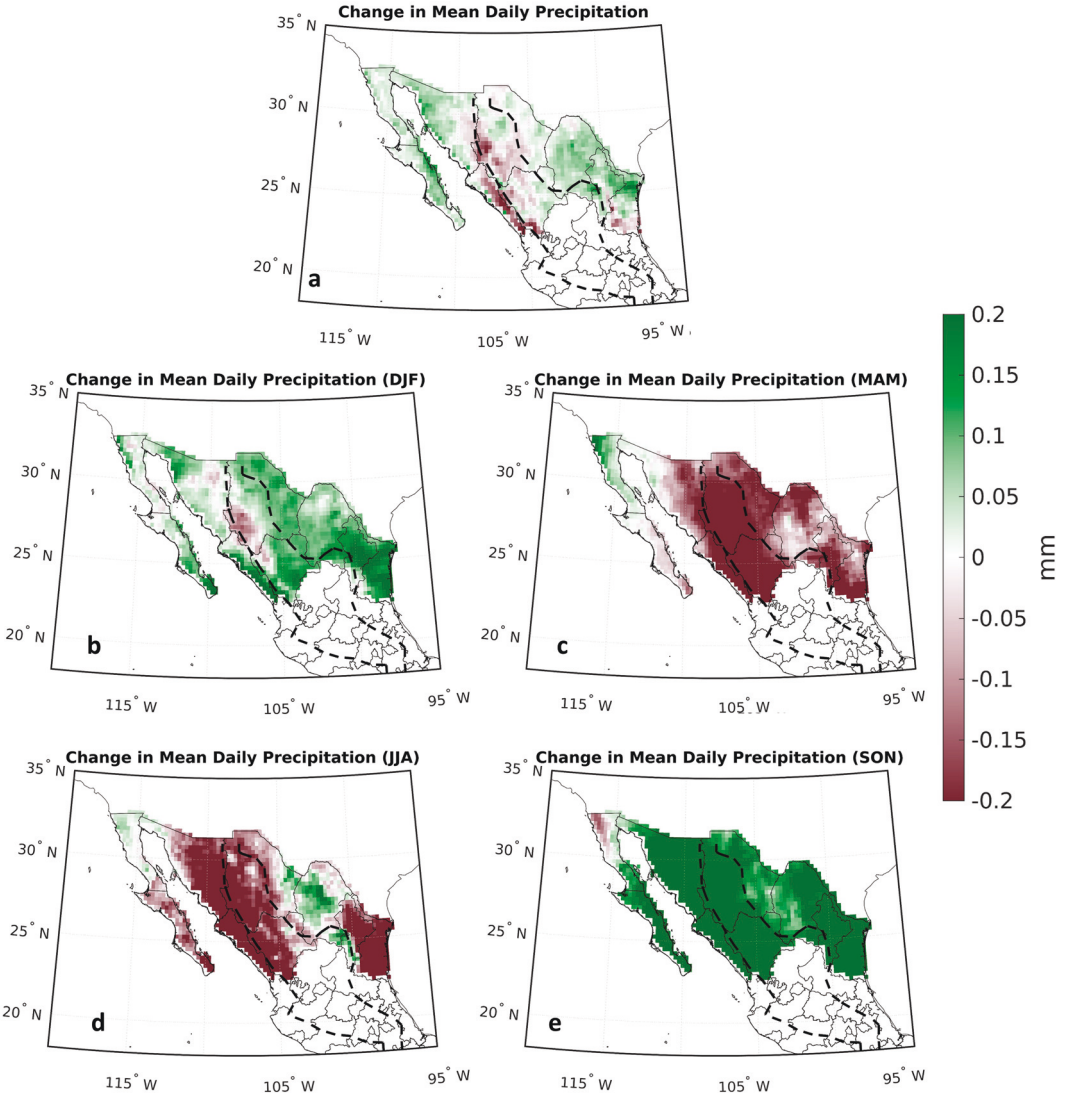

FIG. 4. Ensemble average change (projected minus historical) in (a) annual and (b)–(e) seasonal mean precipitation from NA-CORDEX. The dashed contour delineates the Sierra Madre highlands. We define the historical period as 1986–2005 and the projected period as 2081–2100.

which prior observations indicate a double peak in summertime precipitation (Perdigón-Morales et al. 2018; García-Franco et al. 2021; Colorado-Ruiz and Cavazos 2021) (Fig. 1b). Between these two regions are the dry highlands of central northern Mexico. In the far west of our domain, the Baja California peninsula is extremely dry (precipitation is generally less than 0.5 mm day^{-1}).

In the ensemble mean, the historical NA-CORDEX simulations accurately capture the spatial distributions of annual-mean and R99 daily precipitation when compared to MSWEP observations (Fig. 1), with correlation coefficients (ρ) between observed and simulated mean and R99 of $\rho = 0.966$ and $\rho = 0.893$, respectively. Similar skill is seen for individual seasons in Fig. 2, though model skill in R99 tends to be slightly higher in winter and spring [December–February (DJF) and March–May (MAM)] and lower in summer and fall [June–August (JJA) and September–November (SON)] while the converse is true for model skill in mean precipitation.

Both the RMSE and visual inspection of historical model output and MSWEP data (Figs. 1a,b) suggest that simulated mean precipitation rates are very close to observed rates, with a small dry bias in Coahuila and Tamaulipa. Biases in extreme precipitation differ slightly, featuring an underestimation of R99 throughout most of the region. The dry bias is most pronounced in the California Peninsula and in the central NAM region (Figs. 1c,d). These deficiencies are generally most notable in summer and the best agreement is seen in the winter/spring (Fig. 2). The model underestimation of both mean and extreme precipitation is consistent with earlier modeling studies (Frei et al. 2003).

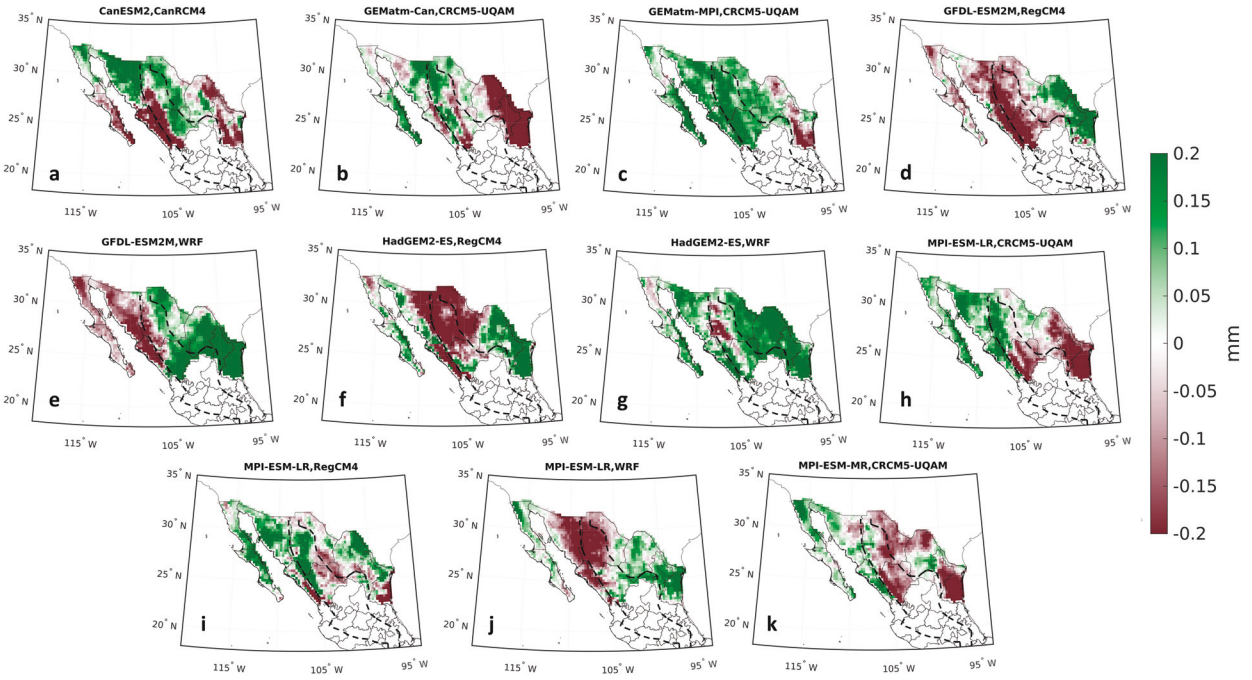

FIG. 5. Change in mean precipitation in the 11 NA-CORDEX ensemble members considered in this analysis. The dashed line delineates the Sierra Madre highlands.

Monthly averages of mean and R99 precipitation over all of northern Mexico (Fig. 3) help further diagnose biases in modeled precipitation. The biases in model-based estimates of the mean daily precipitation are greatest during the beginning of the wet season, during which the model underestimates the magnitude of daily precipitation (note, however, that Fig. 2 illustrates that models capture the spatial pattern of summertime precipitation well). Model estimates of the monthly R99 over northern Mexico are biased high for all seasons except winter (Fig. 3b). Despite these differences, MSWEP-based estimates of mean and extreme precipitation always fall within the 90% confidence intervals (calculated from the intermodel spread) of the historical simulations from the NA-CORDEX ensemble (Figs. 3a,b), except for the month of May for R99. While we caution that precipitation is difficult to observe, Figs. 1–3 demonstrate that the NA-CORDEX simulations capture both the spatial distributions and the seasonality of historical mean and extreme precipitation over northern Mexico with sufficient realism, suggesting that the NA-CORDEX ensemble is a viable tool for studying projected future changes over the region.

4. Projected changes in mean and extreme precipitation

a. Changes in mean precipitation

In the ensemble-mean, NA-CORDEX simulations project a decrease in precipitation where it is presently high and an increase in precipitation where it is presently low (Figs. 4a and 2a–d). Decreases of up to -0.2 mm day^{-1} ($\approx -7\%$) are seen along the western slopes of the Sierra Madre highlands and along the Huasteca region in southern Tamaulipas, and increases of up to $+0.2$ mm day^{-1} are projected for most of Sonora, Coahuila, Baja California, and Nuevo León (Fig. 4a). This is in contrast to temperature, which increases more uniformly over the region (not shown).

Individual simulations in the NA-CORDEX ensemble project changes in mean precipitation of similar magnitudes, but exhibit some diversity in the spatial patterns of change (Fig. 5). Such variation among simulations is largely due to the regional models, as ensemble members with the same driving model exhibit different spatial patterns of change; compare, for example, the simulations using the MPI-ESM-LR global model in Figs. 5h–j.

Examining the changes in the seasonal cycle of precipitation over northern Mexico (Figs. 3a and 4b–e) shows a delay in the arrival of the wet season under the high-emissions scenario. This change results in a drier spring (MAM; Fig. 4b) and summer (JJA; Fig. 4c) with a wetter fall (SON; Fig. 4d), putting additional stress on water resources during some of the warmest months of the year. The reduced mean precipitation along the western edge of the Sierra Madre highlands is consistent with drying of the NAM, which previous studies have discussed (Bukovsky et al. 2015; Pascale et al. 2017; Colorado-Ruiz et al. 2018). We explore the change in NAM characteristics further in section 4c.

Projected precipitation changes outside the NAM region follow a variety of patterns in seasonality and magnitude (Fig. 4). There is substantial intermodel spread in the projections for the northwestern and northeastern corners of the country (Fig. 5), but a seasonal breakdown provides greater clarity. In the northeast corner of our study region (Tamaulipas and Nuevo León), precipitation is projected to increase during fall and winter

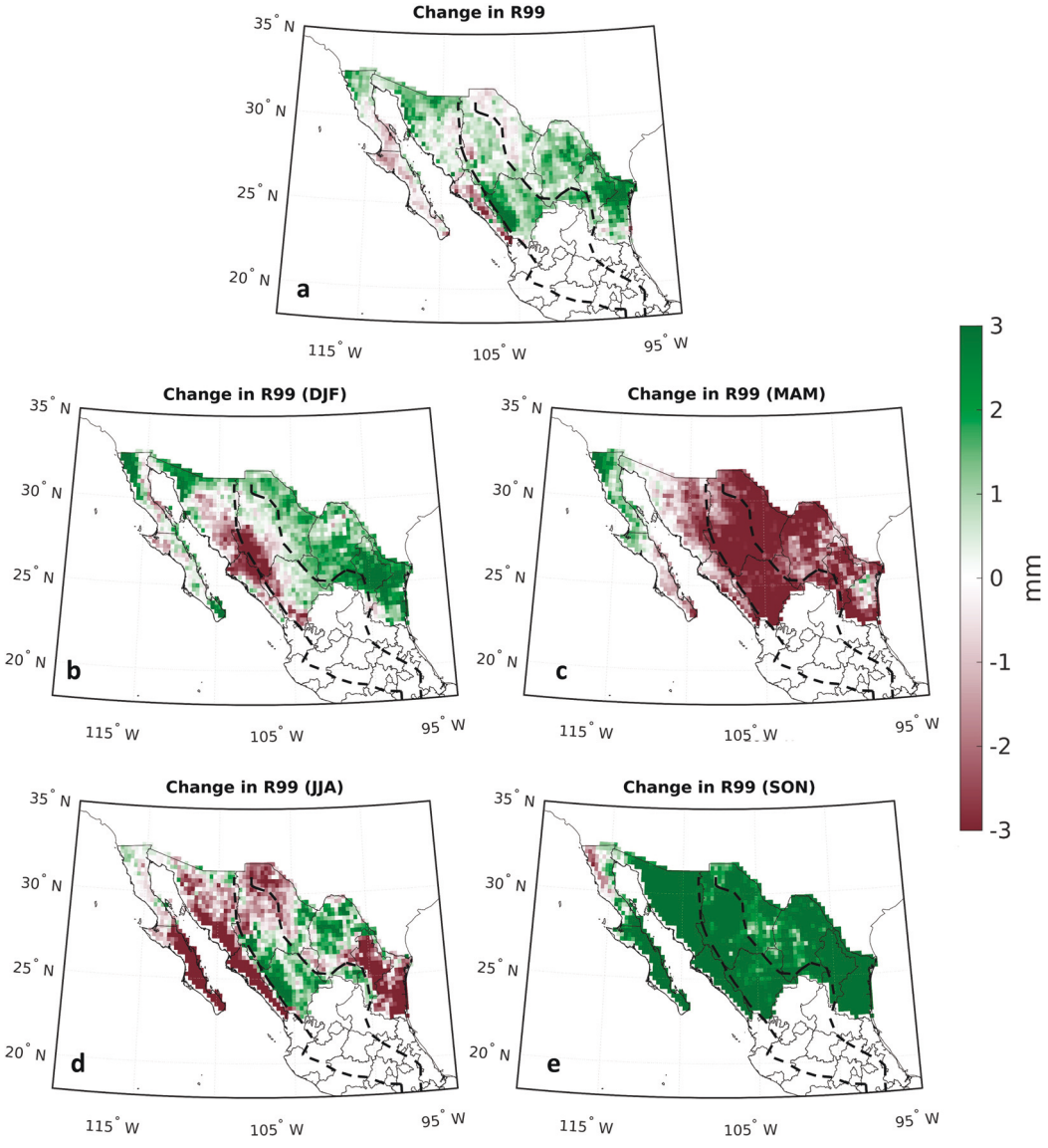

FIG. 6. As in Fig. 4, but for extreme precipitation (R99).

but decrease during spring and summer (Fig. 4). While the NA-CORDEX ensemble reasonably captures the historical precipitation over the region, all ensemble members may not capture the physics responsible for changes in the dynamical drivers of precipitation under global warming. Regional variations in the projected seasonality of precipitation are discussed in section 4d.

b. *Changes in extreme precipitation*

The magnitude of extreme precipitation events is projected to increase during SON and weaken during the MAM (Fig. 6): throughout most of northern Mexico, the magnitude of R99 precipitation events increases by >3 mm day^{-1} during SON (Fig. 6e) and decreases by a similar amount during MAM (Fig. 6c). These changes resemble the seasonal and spatial patterns in projections of mean precipitation (Fig. 4) and could bring about increased risk of flood and water shortages during the wet and dry seasons, respectively.

Projected changes in precipitation extremes show substantial variations across the 11 models considered here (Fig. 7), but agreement across models is better when broken down by season (Fig. 8). Intermodel spread is largest in winter (Fig. 8b) and summer (Fig. 8d), and there is closer agreement for projections of a drier dry season (MAM; Fig. 8c) and a wetter wet season (SON; Fig. 8c). The increased magnitude of R99 during the fall suggests increases in the frequency and/or severity of tropical cyclones originating in the eastern Pacific and North Atlantic basins, and we discuss this in more detail in section 5. Changes in the seasonality of the NAM, such as a later onset and longer duration, could explain

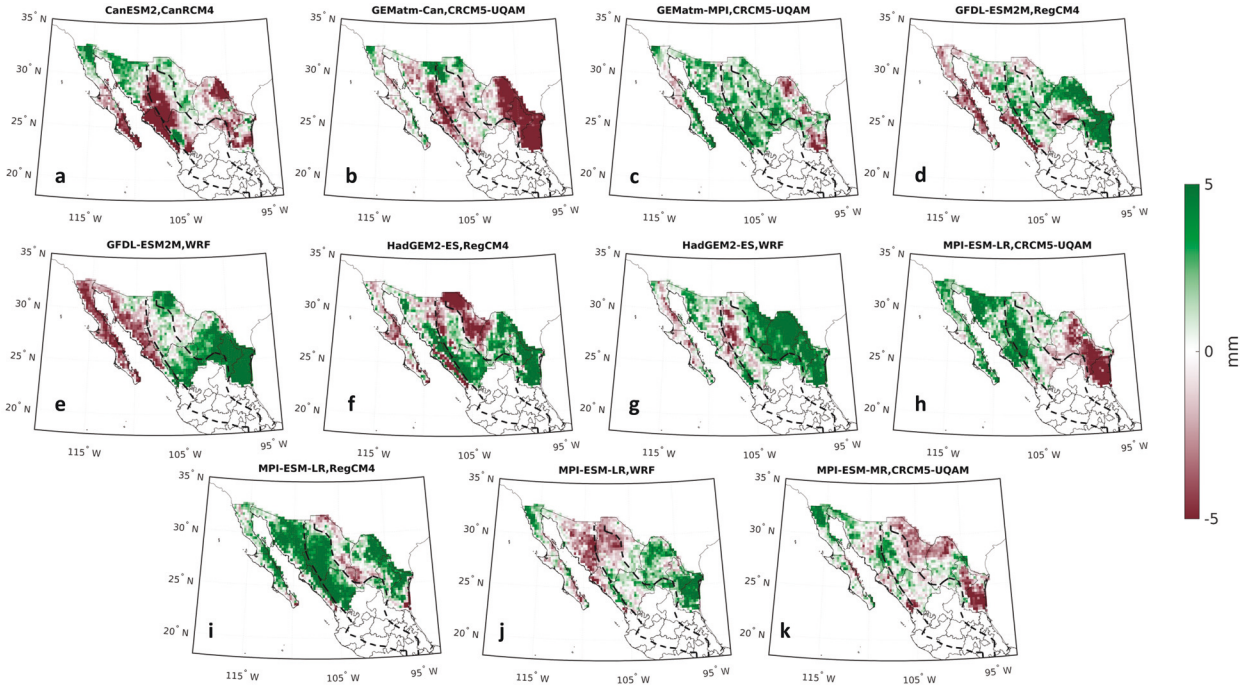

FIG. 7. As in Fig. 5, but for extreme precipitation (R99).

the large increase in fall extreme precipitation; this notion follows results in Ashfaq et al. (2021) and is explored with greater detail in section 4c.

We also consider changes in the frequencies of the strongest storms in Fig. 9 using the same methodology as Nazarian et al. (2022). Projections suggest that moderate storms (i.e., 90th-percentile events) will increase in frequency by approximately 10% per degree of local warming, while the strongest storms (i.e., the 99.99th percentile) will increase in frequency by approximately 20% per degree of local warming. Since the region is projected to warm by approximately 4°C in the multimodel mean, this implies a near-doubling of the frequency of the strongest storms. This is a large increase and is in general agreement with projections for the whole of North America in Zhao et al. (2023). Yet, we note that this increase is much smaller than that in regions such as the northeastern United States (Nazarian et al. 2022) and central Europe (Myhre et al. 2019), which are projected to experience a doubling in frequency per degree of local warming (i.e., 100% $°C^{-1}$) for the strongest storms.

To diagnose the potential drivers of the changes in extreme precipitation over the region, we calculate the fractional changes (Fig. 10). Extreme precipitation is generated by strong updrafts, such that the rate of extreme precipitation (P_e) can be approximated as

$$P_e \approx \int -\rho w \left(\frac{dq_s}{dz}\right) dz, \tag{1}$$

where ρ is the air density, w is the vertical velocity, q_s is the saturation specific humidity, and z is the vertical coordinate (Muller et al. 2011). This expression can be used to decompose fractional changes in P_e as

$$\frac{\delta P_e}{P_e} = \underbrace{\left[\frac{\int \rho w \delta\left(\frac{dq_s}{dz}\right) dz}{\int \rho w \left(\frac{dq_s}{dz}\right) dz}\right]}_{\text{thermodynamic}} + \underbrace{\left[\frac{\int \delta(\rho w)\left(\frac{dq_s}{dz}\right) dz}{\int \rho w \left(\frac{dq_s}{dz}\right) dz}\right]}_{\text{dynamic}} + \underbrace{\left[\frac{\int \delta(\rho w)\delta\left(\frac{dq_s}{dz}\right) dz}{\int \rho w \left(\frac{dq_s}{dz}\right) dz}\right]}_{\text{nonlinear}} \tag{2}$$

where δ is the difference between the projected and historical periods. The thermodynamic contribution to the change in extreme precipitation is based on the Clausius–Clapeyron relation and is approximately +6%–7% $°C^{-1}$. The dynamical contribution to the change in extreme precipitation is smaller in magnitude than the thermodynamic term and is typically ±2% $°C^{-1}$ (O'Gorman 2015). The final term combines nonlinear changes, changes in precipitation efficiency (Lutsko and Cronin 2018; Abbott et al. 2020), and any sources of error, which are typically small.

As previously mentioned, all fractional changes are calculated using the local rate of warming rather than the global rate of warming. We cannot calculate each of the terms in (2) since data are only available at the surface and a few vertical levels, which are insufficient to calculate these vertical integrals. We therefore compare the fractional increases in extreme precipitation with

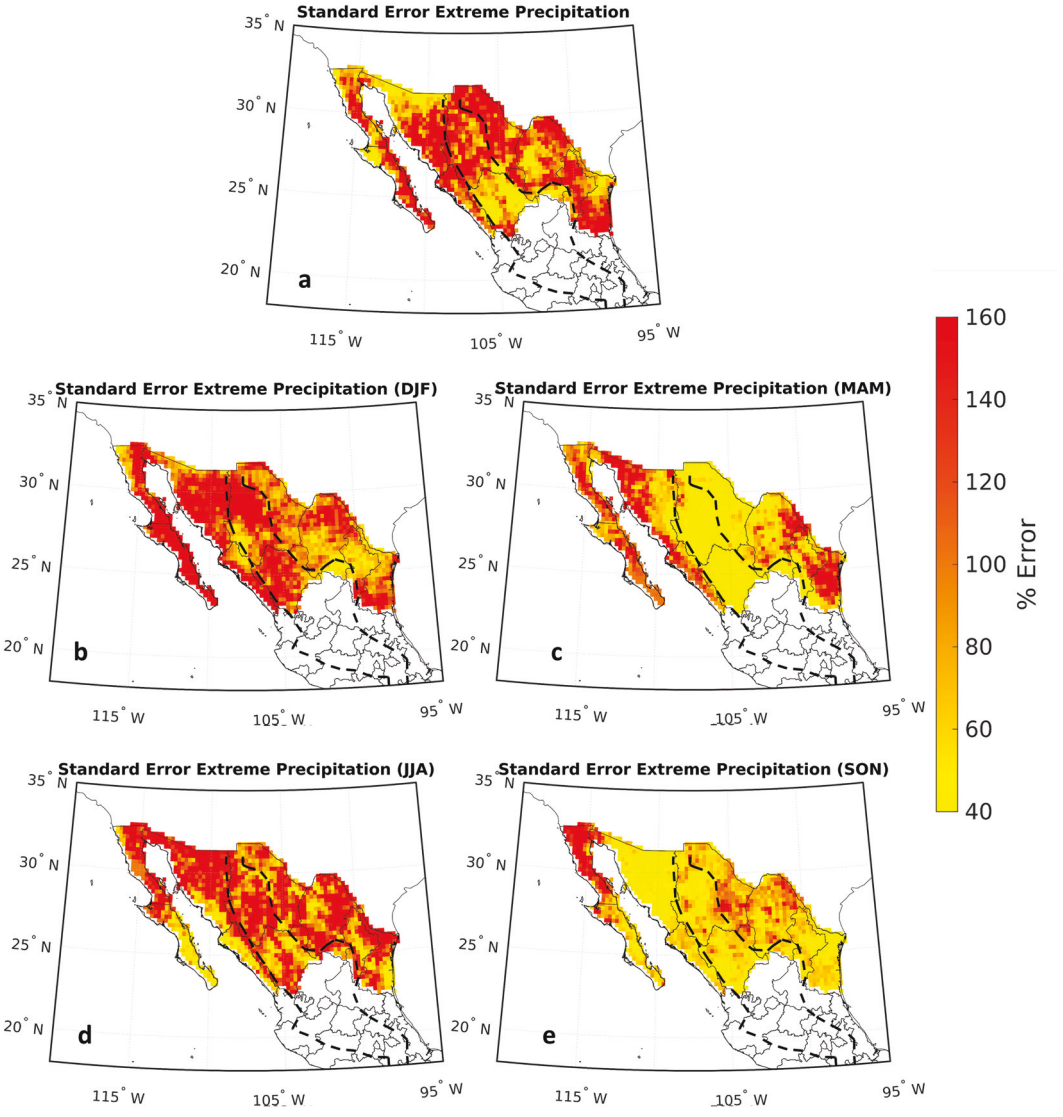

FIG. 8. As in Fig. 6, but for multimodel standard error in the change in extreme precipitation.

the thermodynamic rate of ~6%–7% $°C^{-1}$ and interpret departures from this rate as likely reflecting dynamical changes. We caution however, that departures from Clausius–Clapeyron scaling might also be due to cloud microphysical processes and the representation of such processes in NA-CORDEX (Singh and O'Gorman 2014; Lutsko and Cronin 2018; Abbott et al. 2020) or nonlinear effects.[1]

The fractional change in annual extreme precipitation is small and positive over most of the region, with an average of approximately 2% $°C^{-1}$ (see Figs. 10 and 11). This suggests a strong dynamical damping of changes in extreme precipitation over the region. In addition to the potential dynamical damping of the changes in extreme precipitation, there may be a lack of water availability to support the thermodynamics increase in extreme precipitation. Such analysis is outside the scope of this work, as all of the regions from which the water vapor is sourced are not included in the NA-CORDEX domain. The fractional changes are generally highest in fall (Fig. 10e) but are still below 7% $°C^{-1}$ over the majority of the region. In spring (MAM) fractional decreases of up to −3% $°C^{-1}$ are seen in much of the region. These seasonal changes in the fractional change partly reflect changes in the timing of extreme precipitation due to the monsoon.

c. *Changes in NAM characteristics*

The changes in the seasonality of mean and extreme precipitation seen in Figs. 4 and 6 are likely due at least in part to the changing NAM. To investigate this link, we start by considering the seasonality of precipitation over the states that experience the NAM: Baja California Sur, Sonora, Chihuahua, Sinaloa,

[1] However, consistency across models suggests that changes are likely driven by dynamics rather than microphysics.

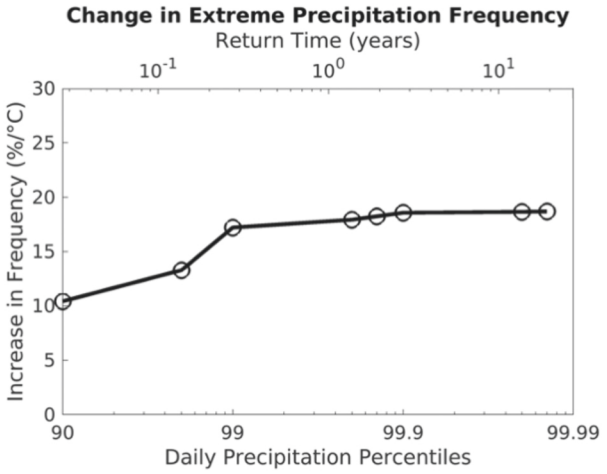

FIG. 9. Change in storm frequency per degree of local warming averaged over the 11 ensemble members. Storm strength is presented as both a percentile (bottom axis) and return time (top axis). The analysis is conducted over the entire northern Mexico domain and using the full 20-yr historical and projected periods.

and Durango. Like Fig. 3, Fig. 12 shows a 2-week delay in the timing of the high precipitation season. The shift in the seasonality of both mean and extreme precipitation over the region also exhibits a longer tail in the fall, with the end period of the monsoon becoming more protracted and less sudden.

The North American monsoon is not the only physical process that contributes to precipitation over this subregion, so we use the Zhang et al. (2002) metric described in section 2 to specifically diagnose changes in the monsoon timing and length. Results are presented in Table 2. Before considering projected changes in the NAM using NA-CORDEX, we compare the simulated historical NAM with observations. NA-CORDEX exhibits an early bias to the monsoon onset (approximately 3 weeks earlier than observations) but captures the end of the monsoon quite well. This leads to a simulated monsoon that is approximately 2 weeks longer than that observed. We note, however, that there is significant variability between ensemble members in their estimates of the NAM timings, with more variability in the NAM start time than in the end time.

Despite the earlier start time in the NAM using CORDEX, the simulations still produce pronounced monsoon seasonality, with which we may calculate changes through the end of the century. By the end of the century, the NAM is projected to start approximately 1 week later, end approximately 3 weeks later, and last approximately 2 weeks longer than the historical period (Table 2). We again note the sizeable spread in the NAM characteristics across simulations, but almost all models suggest a delay in the onset and a lengthening of the monsoon season. The agreement among the NA-CORDEX ensemble members of a delayed NAM onset and retreat, and overall NAM lengthening, is particularly noteworthy given the spread of individual models (see Table 1). The projected delay in the NAM seen in the NA-CORDEX ensemble is similar to that seen in the larger CMIP5 ensemble (Cook and Seager 2013) and several RCMs (Ashfaq et al. 2021) as is the relatively small change in precipitation rates during the monsoon season (Seager and Vecchi 2010), though an increase in extreme monsoonal precipitation is expected. While there is agreement between these results and those in other analyses using the CMIP ensemble, we note that GCMs suffer from SST biases, and such biases have been observed to have an impact on the NAM response (Pascale et al. 2017; Meyer and Jin 2017). The changes in seasonality over the region, considering NAM in the context of other processes responsible for precipitation over the region, are discussed further in section 5.

d. *Case study: Five major cities*

Finally, we have conducted a case study of changes in precipitation over five major cities in northern Mexico: Ciudad Juárez, Monterrey, Culiacán, Hermosillo, and Tijuana (Fig. 13). These cities were chosen because they are all major social and economic hubs and their locations are spread out throughout most of northern Mexico. Therefore, cities shown in Fig. 13 represent a somewhat comprehensive selection of climate regimes in this region and help us best exemplify the variety in timing and intensity of precipitation changes in NA-CORDEX projections.

There are several notable differences in local precipitation changes over these cities compared to the larger regional changes. For example, although precipitation is projected to decrease for summer and increase for fall over most of northern Mexico, drier summers are only evident in Monterrey and Culiacán (Figs. 13b,c), and wetter falls are only projected for Monterrey, Hermosillo, and Tijuana (Figs. 13b,d,e). Precipitation changes over Ciudad Juárez are small (Fig. 13a), while Tijuana is the only city where increased winter precipitation may be expected from the NA-CORDEX projections (Fig. 13e).

Changes in the timing of local precipitation are crucial for urban populations and decision makers. Monterrey is projected to see a reduction in precipitation between late June and September (Fig. 13b), when heat stress and demand on water resources are greatest. Even though the annual mean daily precipitation for Monterrey and its surroundings is projected to only change slightly (Figs. 4a and 13g), the wetter falls that compensate for drier summers can exacerbate risk of flooding that has historically affected the city due to tropical cyclone remnants (Aguilar-Barajas et al. 2019). In Culiacán, drier summers are likely to impact the early growing season and thus shift agricultural activities that sustain the economy of Sinaloa.

Histograms of yearly cumulative precipitation provide more insight into possible challenges facing decision makers in northern Mexican cities (Figs. 13f–j). The frequency of years with lower cumulative precipitation is projected to increase for Ciudad Juárez, Monterrey, and Culiacán (Figs. 13f–h), while high-precipitation years are projected to increase in all cities except Culiacán, where the wettest years are still projected to be wetter than in historical simulations (Fig. 13h). These results are consistent with projected changes in extreme precipitation at the regional level (Fig. 6) and across all of northern

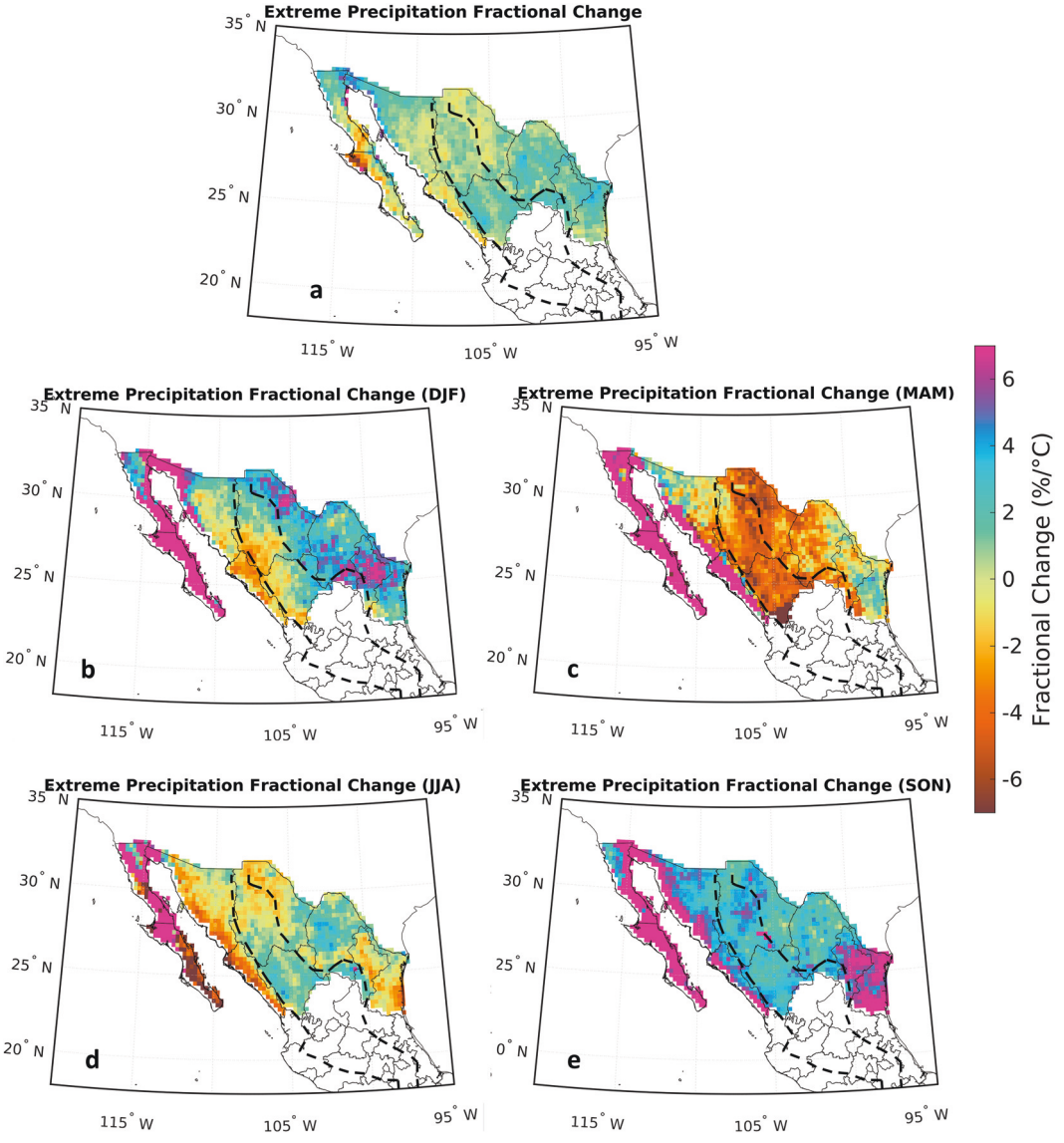

FIG. 10. As in Fig. 6, but for the fractional change in extreme precipitation.

Mexico (Fig. 9), pointing to the disproportionate role of extreme events in future hydrological changes in the region.

5. Discussion and conclusions

Simulations suggest that the spatial pattern of future trends in mean precipitation is strikingly similar to that of extreme precipitation (Figs. 4 and 6). Regions projected to experience a decrease in mean precipitation are likewise projected to experience a decrease in extreme precipitation, and vice versa. While some previous studies based on lower-resolution models failed to resolve these spatial patterns in the sign of projected precipitation changes (Zhao et al. 2023), the magnitudes of these changes are relatively small (approximately 10% for both mean and extreme precipitation) and well below the increase that would be expected from thermodynamics alone (Figs. 10 and 11). However, the frequency of extreme precipitation events is likely to increase by 50%–100%, suggesting that the water the region depends on for agriculture will be more intermittent and management practices will have to adapt accordingly (Fig. 9).

Relatively small changes in annually averaged precipitation mask a significant seasonal change in both mean and extreme precipitation. The largest changes are projected to occur during spring and fall, when precipitation is expected to decrease and increase, respectively, with lower magnitude and regionally dependent changes during winter and summer. This shift in maximum precipitation to later in the year is consistent with a delayed onset of the North American monsoon. While drying is projected to occur in certain regions throughout the year, drying during the summertime is particularly significant

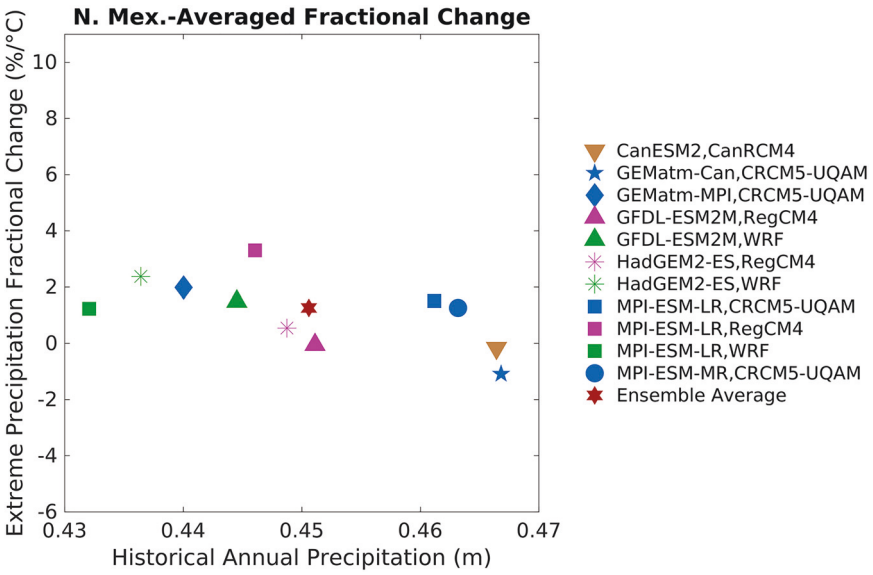

FIG. 11. Fractional changes in ensemble-average extreme precipitation. Each GCM has a unique marker and each RCM has a unique color.

given that northern Mexico already experiences significant heat stress during this time of the year (Hallack-Alegria and Watkins 2007). Chihuahua, Sinaloa, and Sonora, which amount for 72% of northern Mexico's agricultural output (INEGI 2020), are all projected to experience strong drying during the spring and summer months, which would have major implications for northern Mexico's food availability and security. Spring and summer drying were likewise seen in the downscaled simulations of Cavazos and Arriaga-Ramírez (2012), who used an earlier generation of models to analyze changes in precipitation over the subregion of Baja California, as well as Cook and Seager (2013), Torres-Alavez et al. (2014) and Ashfaq et al. (2021), who likewise observed a shift of the monsoon to later in the year, although some studies suggest that this may be due to biases in SST (Pascale et al. 2017). While we cannot diagnose the cause of the delay here due to the lack of data in the vertical, earlier studies highlight the role of atmospheric stability due to tropospheric warming, with Pascale et al. (2017) suggesting an overall drying in the NAM due to increased stability, while Cook and Seager (2013) suggests that this increase in early summer stability is finally overcome by moisture convergence which triggers the delayed NAM onset.

The projected large, widespread decreases in seasonal precipitation (Figs. 4b–e) are likely to further stress northern Mexican water resources and public health infrastructure. For example, historical records have shown a positive association between fall and winter precipitation rates and the incidence of dengue fever in the region (Brunkard et al. 2008). The increases in both mean and extreme precipitation over northern Mexico seen here, as well as the projected warming, suggest that the environment may become conducive to the spread of dengue fever through the end of the century (Chowell and Sanchez 2006).

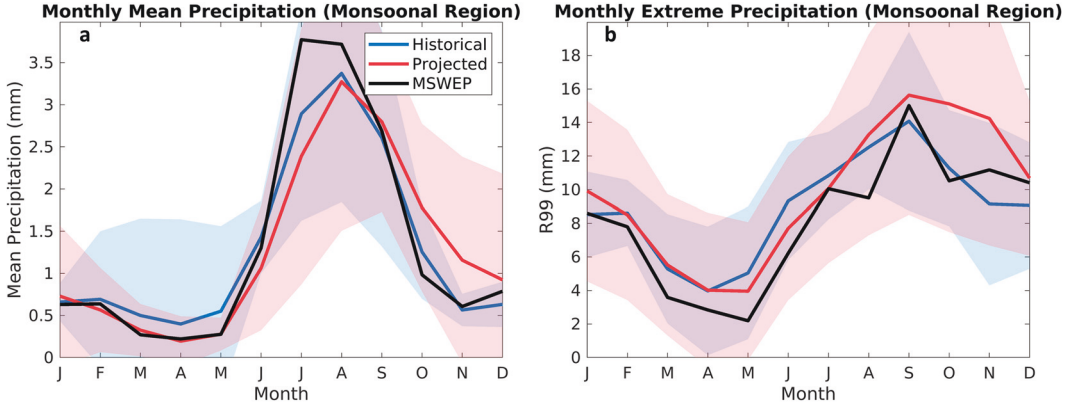

FIG. 12. As in Fig. 3, but considering just the states that experience that NAM.

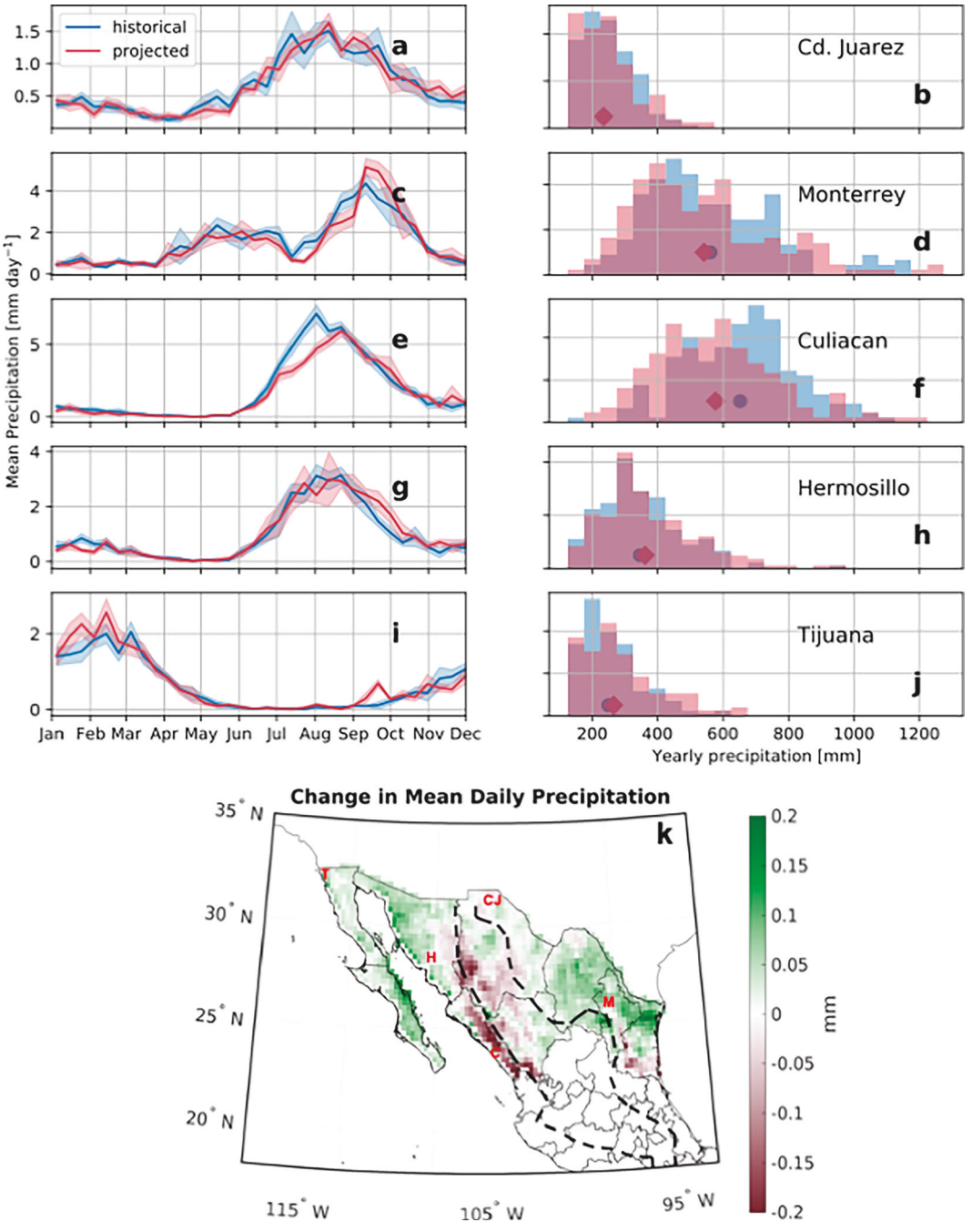

FIG. 13. Changes in precipitation in major metropolitan areas. (a),(c),(e),(g),(i) For each city, multimodel averages of daily precipitation throughout the year are shown with 90% confidence intervals in shading. (b),(d),(f),(h)(j) Histograms of accumulated yearly precipitation for the two 20-yr periods considered in this study are shown in color. The circles and diamonds at the bottom of each histogram represent the mean historical and projected values, respectively. (k) The location of each city is shown superimposed on the plot of the change in mean daily precipitation.

Some of the changes in precipitation, particularly over the western states during late spring and summer, are likely due to changes in the North American monsoon. Based on the NA-CORDEX ensemble, the NAM is projected to begin and end later and last longer, thereby shifting and extending the period of heavy rainfall later in the year. This shift may exacerbate drought conditions that typically peak before the NAM in the state of Sonora, particularly given the high heat stress and demand for water resources during the spring (Hallack-Alegria and Watkins

TABLE 2. Comparison of North American monsoon statistics in MSWEP and NA-CORDEX simulations, as calculated with the modified Zhang et al. (2002) metric. Statistics for historical and projected periods are denoted by H and P, respectively. The final column indicates the change in the ensemble average (projected minus historical) and indicates that the NAM is expected to start and end later, and last longer.

	MSWEP	Ensemble average (H)	Standard error (H)	Ensemble average (P)	Standard error (P)	Change
Start	26 Jun	5 Jun	16 days	12 Jun	18 days	+7 days
End	24 Sep	16 Sep	13 days	7 Oct	10 days	+21 days
Length	90 days	103 days	16 days	117 days	22 days	+14 days

2007). Furthermore, other studies have shown that, even if the precipitation were to remain fixed, the increased temperature alone could exacerbate drought conditions over some of the region (Ault et al. 2016). While there is reasonable agreement between the simulations in the shift of the monsoon later in the year with results from earlier studies (Cook and Seager 2013), there are significant model differences in the timing of the end of the monsoon. Follow-up studies to more precisely quantify the shift of the NAM using a larger ensemble and to investigate other potential mechanisms that may be responsible for the spring changes (Seth et al. 2011) may be advantageous.

While much of the focus here has been on changes in late spring, summer, and fall precipitation due to the delay in the NAM, we note that the winter precipitation has been shown in the literature to be closely tied to ENSO, with more (less) wintertime precipitation during the El Niño (La Niña) phase (Magaña et al. 2003; Mendoza et al. 2005; Englehart and Douglas 2006; Cabrera et al. 2010). A future investigation of the trend in ENSO state in NA-CORDEX is warranted, as biases in the projection of the phases of ENSO has nonnegligible ramifications for projections of wintertime precipitation over this region.

Furthermore, an increase in the rain rate of future Atlantic tropical cyclones, particularly those that propagate over or near northern Mexico, may be responsible for the increase in extreme precipitation during the fall, as seen in Knutson et al. (2020). Given that the primary genesis regions in the eastern North Pacific and Atlantic regions are outside of the NA-CORDEX domain (Tippett et al. 2011), the NA-CORDEX ensemble has nonnegligible bias in its projections of mean and extreme precipitation, and this bias is particularly large for the western coast of Mexico (Rendfrey et al. 2021). Despite this bias, the projected increase in tropical cyclone–driven precipitation over the region is consistent with Dominguez et al. (2021). Based on our results, we hypothesize that the extension of the NAM, which primarily impacts the western portion of the region, coupled with the increase in tropical cyclone precipitation from Atlantic tropical cyclones over the eastern portion of the region may be responsible for the projected increase in mean and extreme precipitation across the region during fall.

While we have conducted a comprehensive study of the future trends in mean and extreme precipitation over northern Mexico through the end of the century, we have not been able to identify the dynamical drivers responsible for these trends. A follow-up study analyzing the change in circulation patterns over the region is essential to provide a full understanding of the physical processes driving this change. Based on the results presented here, we expect that there is a significant slowdown of the dynamics driving changes in precipitation (particularly extreme precipitation) over this region. Nevertheless, the analysis presented here is an important and necessary first step in quantifying changes in the hydroclimate of northern Mexico, which is required for stakeholders and local agencies to prepare for the increased intermittency and significant seasonal changes in precipitation over this important yet understudied region.

Acknowledgments. The authors thank Dr. Jorge García-Franco and three anonymous reviewers for providing helpful feedback on an earlier version of this manuscript. R. Nazarian, B. Matijevic, J. Vizzard, and C. Agostino gratefully acknowledge support from Fairfield University, including the College of Arts and Sciences, Science Institute, and Provost's Office. R. Nazarian, B. Matijevic, J. Vizzard, and C. Agostino also gratefully acknowledge support from the NASA Connecticut Space Grant Consortium, award P-1704. N. Brizuela was supported by Consejo Nacional de Ciencia y Tecnología and UC Mexus. N. Lutsko was supported by NSF grant OCE-2023483. More information about conducting undergraduate research with CORDEX can be found in Nazarian (2021).

Data availability statement. All NA-CORDEX simulations used in this study are freely available on the NCAR Climate Data Gateway: https://www.earthsystemgrid.org/search/cordexsearch.html. All MSWEP data are freely available on the GloH2O portal: https://www.gloh2o.org/mswep/.

REFERENCES

Abbott, T. H., T. W. Cronin, and T. Beucler, 2020: Convective dynamics and the response of precipitation extremes to warming in radiative–convective equilibrium. *J. Atmos. Sci.*, **77**, 1637–1660, https://doi.org/10.1175/JAS-D-19-0197.1.

Adams, D. K., and A. C. Comrie, 1997: The North American monsoon. *Bull. Amer. Meteor. Soc.*, **78**, 2197–2214, https://doi.org/10.1175/1520-0477(1997)078<2197:TNAM>2.0.CO;2.

Aguilar-Barajas, I., N. P. Sisto, A. I. Ramirez, and V. Magaña-Rueda, 2019: Building urban resilience and knowledge coproduction in the face of weather hazards: Flash floods in the Monterrey metropolitan area (Mexico). *Environ. Sci. Policy*, **99**, 37–47, https://doi.org/10.1016/j.envsci.2019.05.021.

Almazroui, M., and Coauthors, 2021: Projected changes in temperature and precipitation over the United States, Central America, and the Caribbean in CMIP6 GCMs. *Earth Syst. Environ.*, **5** (1), 1–24, https://doi.org/10.1007/s41748-021-00199-5.

Andrews, T., J. M. Gregory, M. J. Webb, and K. E. Taylor, 2012: Forcing, feedbacks and climate sensitivity in CMIP5 couples atmosphere-ocean climate models. *Geophys. Res. Lett.*, **39**, L09712, https://doi.org/10.1029/2012GL051607.

Ashfaq, M., D. Rastogi, R. Mei, S.-C. Kao, S. Gangrade, B. S. Naz, and D. Touma, 2016: High-resolution ensemble projections of near-term regional climate over the continental United States. *J. Geophys. Res. Atmos.*, **121**, 9943–9963, https://doi.org/10.1002/2016JD025285.

——, and Coauthors, 2021: Robust late twenty-first century shift in the regional monsoons in RegCM-CORDEX simulations. *Climate Dyn.*, **57**, 1463–1488, https://doi.org/10.1007/s00382-020-05306-2.

Ault, T. R., J. S. Mankin, B. I. Cook, and J. E. Smerdon, 2016: Relative impacts of mitigation, temperature, and precipitation on 21st-century megadrought risk in the American Southwest. *Sci. Adv.*, **2**, e1600873, https://doi.org/10.1126/sciadv.1600873.

Ban, N., J. Schmidli, and C. Schär, 2015: Heavy precipitation in a changing climate: Does short-term summer precipitation increase faster? *Geophys. Res. Lett.*, **42**, 1165–1172, https://doi.org/10.1002/2014GL062588.

Barlow, M., S. Nigam, and E. H. Berbery, 1998: Evolution of the North American monsoon system. *J. Climate*, **11**, 2238–2257, https://doi.org/10.1175/1520-0442(1998)011<2238:EOTNAM>2.0.CO;2.

Beck, H. E., and Coauthors, 2017: Global-scale evaluation of 22 precipitation datasets using gauge observations and hydrological modeling. *Hydrol. Earth Syst. Sci.*, **21**, 6201–6217, https://doi.org/10.5194/hess-21-6201-2017.

——, E. F. Wood, M. Pan, C. K. Fisher, D. G. Miralles, A. I. J. M. van Dijk, T. R. McVicar, and R. F. Adler, 2019: MSWEP V2 global 3-hourly 0.1° precipitation: Methodology and quantitative assessment. *Bull. Amer. Meteor. Soc.*, **100**, 473–500, https://doi.org/10.1175/BAMS-D-17-0138.1.

Boos, W. R., and S. Pascale, 2021: Mechanical forcing of the North American monsoon by orography. *Nature*, **599**, 611–615, https://doi.org/10.1038/s41586-021-03978-2.

Breña Naranjo, J. A., A. Pedrozo-Acuña, O. Pozos-Estrada, S. A. Jiménez-López, and M. R. López-López, 2015: The contribution of tropical cyclones to rainfall in Mexico. *Phys. Chem. Earth*, **83–84**, 111–122, https://doi.org/10.1016/j.pce.2015.05.011.

Brunkard, J. M., E. Cifuentes, and S. J. Rothenberg, 2008: Assessing the roles of temperature, precipitation, and ENSO in dengue re-emergence on the Texas-Mexico border region. *Salud Publica Mex.*, **50**, 227–234, https://doi.org/10.1590/S0036-36342008000300006.

Bukovsky, M. S., and L. O. Mearns, 2020: Regional climate change projections from NA-CORDEX and their relation to climate sensitivity. *Climatic Change*, **162**, 645–665, https://doi.org/10.1007/s10584-020-02835-x.

——, C. M. Carrillo, D. J. Gochis, D. M. Hammerling, R. R. McCrary, and L. O. Mearns, 2015: Toward assessing NARCCAP regional climate model credibility for the North American monsoon: Future climate simulations. *J. Climate*, **28**, 6707–6728, https://doi.org/10.1175/JCLI-D-14-00695.1.

Cabrera, J. L. B., E. A. Romero, V. C. Z. Such, C. G. García, and F. E. Porrúa, 2010: Significance tests for the relationship between "El Niño" phenomenon and precipitation in Mexico. *Int. Geophys.*, **49**, 245–261, https://doi.org/10.22201/igeof.00167169p.2010.49.4.132.

Cannon, A. J., 2018: Multivariate quantile mapping bias correction: An *N*-dimensional probability density function transform for climate model simulations of multiple variables. *Climate Dyn.*, **50**, 31–49, https://doi.org/10.1007/s00382-017-3580-6.

Caparas, M., Z. Zobel, A. D. A. Castanho, and C. R. Schwalm, 2021: Increasing risks of crop failure and water scarcity in global breadbaskets by 2030. *Environ. Res. Lett.*, **16**, 104013, https://doi.org/10.1088/1748-9326/ac22c1.

Cavazos, T., 1997: Downscaling large-scale circulation to local winter rainfall in north-eastern Mexico. *Int. J. Climatol.*, **17**, 1069–1082, https://doi.org/10.1002/(SICI)1097-0088(199708)17:10<1069::AID-JOC183>3.0.CO;2-I.

——, and S. Arriaga-Ramírez, 2012: Downscaled climate change scenarios for Baja California and the North American monsoon during the twenty-first century. *J. Climate*, **25**, 5904–5915, https://doi.org/10.1175/JCLI-D-11-00425.1.

——, R. Luna-Niño, R. Cerezo-Mota, R. Fuentes-Franco, M. Méndez, L. F. P. Martínez, and E. Valenzuela, 2019: Climatic trends and regional climate models intercomparison over the CORDEX-CAM (Central America, Caribbean, and Mexico) domain. *Int. J. Climatol.*, **40**, 1396–1420, https://doi.org/10.1002/joc.6276.

Chowell, G., and F. Sanchez, 2006: Climate-based descriptive models of dengue fever: The 2002 epidemic in Colima, Mexico. *J. Environ. Health*, **68**, 40–44, http://www.jstor.org/stable/44527609.

Colorado-Ruiz, G., and T. Cavazos, 2021: Trends of daily extreme and non-extreme rainfall indices and intercomparison with different gridded data sets over Mexico and the southern United States. *Int. J. Climatol.*, **41**, 5406–5430, https://doi.org/10.1002/joc.7225.

——, ——, J. A. Salinas, P. De Grau, and R. Ayala, 2018: Climate change projections from Coupled Model Intercomparison Project phase 5 multi-model weighted ensembles for Mexico, the North American monsoon, and the mid-summer drought region. *Int. J. Climatol.*, **38**, 5699–5716, https://doi.org/10.1002/joc.5773.

Cook, B. I., and R. Seager, 2013: The response of the North American monsoon to increased greenhouse gas forcing. *J. Geophys. Res. Atmos.*, **118**, 1690–1699, https://doi.org/10.1002/jgrd.50111.

Díaz Caravantes, R. E., A. L. Castro Luque, and P. Aranda Gallegos, 2014: Mortalidad por calor natural excesivo en el noroeste de México: Condicionantes sociales asociados a esta causa de muerte. *Front. Norte*, **26**, 155–177.

Diem, J. E., D. P. Brown, and J. McCann, 2012: Multi-decadal changes in the North American monsoon anticyclone. *Int. J. Climatol.*, **33**, 2274–2279, https://doi.org/10.1002/joc.3576.

Diffenbaugh, N. S., J. S. Pal, R. J. Trapp, and F. Giorgi, 2005: Fine-scale processes regulate the response of extreme events to global climate change. *Proc. Natl. Acad. Sci. USA*, **102**, 15 774–15 778, https://doi.org/10.1073/pnas.0506042102.

Di Luca, A., R. de Elia, and R. Laprise, 2012: Potential for added value in precipitation simulated by high-resolution nested regional climate models and observations. *Climate Dyn.*, **38**, 1229–1247, https://doi.org/10.1007/s00382-011-1068-3.

Dominguez, C., J. M. Done, and C. L. Bruyère, 2021: Future changes in tropical cyclone and easterly wave characteristics over tropical North America. *Oceans*, **2**, 429–447, https://doi.org/10.3390/oceans2020024.

Donat, M. G., A. L. Lowry, L. V. Alexander, P. A. O'Gorman, and N. Maher, 2016: More extreme precipitation in the world's dry

and wet regions. *Nat. Climate Change*, **6**, 508–513, https://doi.org/10.1038/nclimate2941.

Englehart, P. J., and A. V. Douglas, 2006: Defining intraseasonal rainfall variability within the North American monsoon. *J. Climate*, **19**, 4243–4253, https://doi.org/10.1175/JCLI3852.1.

Flato, G., and Coauthors, 2013: Evaluation of climate models. *Climate Change 2013: The Physical Science Basis*, T. F. Stocker et al., Eds., Cambridge University Press, 741–866.

Frei, C., J. Christensen, M. Déqué, D. Jacob, R. G. Jones, and P. L. Vidale, 2003: Daily precipitation statistics in regional climate models: Evaluation and intercomparison for the European Alps. *J. Geophys. Res.*, **108**, 4124, https://doi.org/10.1029/2002JD002287.

García-Franco, J. L., S. Osprey, and L. J. Gray, 2021: A wavelet transform method to determine monsoon onset and retreat from precipitation time-series. *Int. J. Climatol.*, **41**, 5295–5317, https://doi.org/10.1002/joc.7130.

Geil, K. L., Y. L. Serra, and X. Zeng, 2013: Assessment of CMIP5 model simulations of the North American monsoon system. *J. Climate*, **26**, 8787–8801, https://doi.org/10.1175/JCLI-D-13-00044.1.

Giorgi, F., and W. J. Gutowski Jr., 2015: Regional dynamical downscaling and the CORDEX initiative. *Annu. Rev. Environ. Resour.*, **40**, 467–490, https://doi.org/10.1146/annurev-environ-102014-021217.

Gochis, D. J., L. Brito-Castillo, and W. J. Shuttleworth, 2006: Hydroclimatology of the North American monsoon region in northwest Mexico. *J. Hydrol.*, **316**, 53–70, https://doi.org/10.1016/j.jhydrol.2005.04.021.

Gutiérrez-Ruacho, O. G., L. Brito-Castillo, S. C. Díaz-Castro, and C. J. Watts, 2010: Trends in rainfall and extreme temperatures in northwestern Mexico. *Climate Res.*, **42**, 133–142, https://doi.org/10.3354/cr00874.

Hallack-Alegria, M., and D. Watkins Jr., 2007: Annual and warm season drought intensity–duration–frequency analysis for Sonora, Mexico. *J. Climate*, **20**, 1897–1909, https://doi.org/10.1175/JCLI4101.1.

Hastings, J. R., and R. Turner, 1965: Seasonal precipitation regimes in Baja California, Mexico. *Geogr. Ann.*, **47**, 204–223, https://doi.org/10.1080/04353676.1965.11879720.

He, C., T. Li, and W. Zhou, 2020: Drier North American monsoon in contrast to Asian–African monsoon under global warming. *J. Climate*, **33**, 9801–9816, https://doi.org/10.1175/JCLI-D-20-0189.1.

INEGI, 2020: Encuesta nacional agropecuaria 2019. INEGI Tech. Doc., 32 pp., https://www.inegi.org.mx/rnm/index.php/catalog/607/related_materials?idPro=.

Jáuregui, E., 2003: Climatology of landfalling hurricanes and tropical storms in Mexico. *Atmósfera*, **16**, 193–204.

Kirchmeier-Young, M. C., F. W. Zwiers, N. P. Gillett, and A. J. Cannon, 2017: Attributing extreme fire risk in western Canada to human emissions. *Climatic Change*, **144**, 365–379, https://doi.org/10.1007/s10584-017-2030-0.

Knutson, T., and Coauthors, 2020: Tropical cyclones and climate change assessment: Part II: Projected response to anthropogenic warming. *Bull. Amer. Meteor. Soc.*, **101**, E303–E322, https://doi.org/10.1175/BAMS-D-18-0194.1.

Lahmers, T. M., C. L. Castro, D. K. Adams, Y. L. Serra, J. J. Brost, and T. Luong, 2016: Long-term changes in the climatology of transient inverted troughs over the North American monsoon region and their effects on precipitation. *J. Climate*, **29**, 6037–6064, https://doi.org/10.1175/JCLI-D-15-0726.1.

Leung, L. R., L. O. Mearns, F. Giorgi, and R. L. Wilby, 2003: Regional climate research: Needs and opportunities. *Bull. Amer. Meteor. Soc.*, **84**, 89–95, https://doi.org/10.1175/BAMS-84-1-89.

Li, L., Y. Wang, L. Wang, Q. Hu, Z. Zhu, L. Li, and C. Li, 2022: Spatio-temporal accuracy evaluation of MSWEP daily precipitation over the Huaihe River Basin, China: A comparison study with representative satellite- and reanalysis-based products. *J. Geogr. Sci.*, **32**, 2271–2290, https://doi.org/10.1007/s11442-022-2047-9.

Lopez-Cantu, T., A. F. Prein, and C. Samaras, 2020: Uncertainties in future U.S. extreme precipitation from downscaled climate projections. *Geophys. Res. Lett.*, **47**, e2019GL086797, https://doi.org/10.1029/2019GL086797.

Lucas-Picher, P., R. Laprise, and K. Winger, 2017: Evidence of added value in North American regional climate model hindcast simulations using ever-increasing horizontal resolutions. *Climate Dyn.*, **48**, 2611–2633, https://doi.org/10.1007/s00382-016-3227-z.

Luna-Niño, R., T. Cavazos, J. A. Torres-Alavez, F. Giorgi, and E. Coppola, 2021: Interannual variability of the boreal winter subtropical jet stream and teleconnections over the CORDEX-CAM domain during 1980–2010. *Climate Dyn.*, **57**, 1571–1594, https://doi.org/10.1007/s00382-020-05509-7.

Luong, T. M., C. L. Castro, H.-I. Chang, T. Lahmers, D. K. Adams, and C. A. Ochoa-Moya, 2017: The more extreme nature of North American monsoon precipitation in the southwestern United States as revealed by a historical climatology of simulated severe weather events. *J. Appl. Meteor. Climatol.*, **56**, 2509–2529, https://doi.org/10.1175/JAMC-D-16-0358.1.

Lutsko, N. J., and T. W. Cronin, 2018: Increase in precipitation efficiency with surface warming in radiative-convective equilibrium. *J. Adv. Model. Earth Syst.*, **10**, 2992–3010, https://doi.org/10.1029/2018MS001482.

Magaña, V. O., J. L. Vázquez, J. L. Pérez, and J. B. Pérez, 2003: Impact of El Niño on precipitation in Mexico. *Geofis. Int.*, **42**, 313–330, https://doi.org/10.22201/igeof.00167169p.2003.42.3.949.

——, E. Herrera, C. J. Ábrego-Góngora, and J. A. Ávalos, 2021: Socioeconomic drought in a Mexican semi-arid city: Monterrey metropolitan area, a case study. *Front. Water*, **3**, 579564, https://doi.org/10.3389/frwa.2021.579564.

Martinez-Villalobos, C., and J. D. Neelin, 2019: Why do precipitation intensities tend to follow gamma distributions? *J. Atmos. Sci.*, **76**, 3611–3631, https://doi.org/10.1175/JAS-D-18-0343.1.

McGinnis, S., and L. Mearns, 2021: Building a climate service for North America based on the NA-CORDEX data archive. *Climate Serv.*, **22**, 100233, https://doi.org/10.1016/j.cliser.2021.100233.

Mendoza, B., E. Jáuregui, R. Diaz-Sandoval, V. García-Acosta, V. Velasco, and G. Cordero, 2005: Historical droughts in Central Mexico and their relation with El Niño. *J. Appl. Meteor.*, **44**, 709–716, https://doi.org/10.1175/JAM2210.1.

Meyer, J. D. D., and J. Jin, 2017: The response of future projections of the North American monsoon when combining dynamical downscaling and bias correction of CCSM4 output. *Climate Dyn.*, **49**, 433–447, https://doi.org/10.1007/s00382-016-3352-8.

Muller, C., and Y. Takayabu, 2020: Response of precipitation extremes to warming: What have we learned from theory and idealized cloud-resolving simulations, and what remains to be learned? *Environ. Res. Lett.*, **15**, 035001, https://doi.org/10.1088/1748-9326/ab7130.

——, P. A. O'Gorman, and L. E. Back, 2011: Intensification of precipitation extremes with warming in a cloud-resolving model. *J. Climate*, **24**, 2784–2800, https://doi.org/10.1175/2011JCLI3876.1.

Myhre, G., and Coauthors, 2019: Frequency of extreme precipitation increases extensively with event rareness under global warming. *Sci. Rep.*, **9**, 16063, https://doi.org/10.1038/s41598-019-52277-4.

Nazarian, R. H., 2021: The use of model intercomparison projects in engaging undergraduates in climate change research. *Scholarship Pract. Undergrad. Res.*, **5**, 27–30, https://doi.org/10.18833/spur/5/1/8.

——, J. V. Vizzard, C. P. Agostino, and N. J. Lutsko, 2022: Projected changes in future extreme precipitation over the northeast United States in the NA-CORDEX ensemble. *J. Appl. Meteor. Climatol.*, **61**, 1649–1668, https://doi.org/10.1175/JAMC-D-22-0008.1.

O'Gorman, P. A., 2015: Precipitation extremes under climate change. *Curr. Climate Change Rep.*, **1**, 49–59, https://doi.org/10.1007/s40641-015-0009-3.

Ortega-Gaucin, D., and I. Velasco, 2013: Aspectos socioeconómicos y ambientales de las Sequías en México. *Aqua-LAC*, **5**, 78–90, https://doi.org/10.29104/phi-aqualac/2013-v5-2-08.

Pascale, S., W. R. Boos, S. Bordoni, T. L. Delworth, S. B. Kapnick, H. Murakami, G. A. Vecchi, and W. Zhang, 2017: Weakening of the North American monsoon with global warming. *Nat. Climate Change*, **7**, 806–812, https://doi.org/10.1038/nclimate3412.

——, L. M. V. Carvalho, D. K. Adams, C. L. Castro, and I. F. A. Cavalcanti, 2019: Current and future variations of the monsoons of the Americas in a warming climate. *Curr. Climate Change Rep.*, **5**, 125–144, https://doi.org/10.1007/s40641-019-00135-w.

Pendergrass, A. G., F. Lehner, B. M. Sanderson, and Y. Xu, 2015: Does extreme precipitation intensity depend on the emission scenario? *Geophys. Res. Lett.*, **42**, 8767–8774, https://doi.org/10.1002/2015GL065854.

Perdigón-Morales, J., R. Romero-Centeno, P. O. Pérez, and B. S. Barrett, 2018: The midsummer drought in Mexico: Perspectives on duration and intensity from the CHIRPS precipitation database. *Int. J. Climatol.*, **38**, 2174–2186, https://doi.org/10.1002/joc.5322.

Prein, A. F., R. M. Rasmussen, K. Ikeda, C. Liu, M. P. Clark, and G. J. Holland, 2017: The future intensification of hourly precipitation extremes. *Nat. Climate Change*, **7**, 48–52, https://doi.org/10.1038/nclimate3168.

Rajczak, J., P. Pall, and C. Schär, 2013: Projections of extreme precipitation events in regional climate simulations for Europe and the Alpine region. *J. Geophys. Res. Atmos.*, **118**, 3610–3626, https://doi.org/10.1002/jgrd.50297.

Ramos-Pérez, O., D. K. Adams, C. A. Ochoa-Moya, and A. I. Quintanar, 2022: A climatology of mesoscale convective systems in northwest Mexico during the North American monsoon. *Atmosphere*, **13**, 665, https://doi.org/10.3390/atmos13050665.

Rendfrey, T. S., M. S. Bukovsky, R. R. McCrary, and R. Fuentes-Franco, 2021: An assessment of tropical cyclones in North American CORDEX WRF simulations. *Wea. Climate Extremes*, **34**, 100382, https://doi.org/10.1016/j.wace.2021.100382.

Reyes, S., M. W. Douglas, and R. A. Maddox, 1994: El monzón del suroeste de Norteamérica (TRAVASON/SWAMP). *Atmósfera*, **7**, 117–137.

Schär, C., and Coauthors, 2016: Percentile indices for assessing changes in heavy precipitation events. *Climatic Change*, **137**, 201–216, https://doi.org/10.1007/s10584-016-1669-2.

Seager, R., and G. A. Vecchi, 2010: Greenhouse warming and the 21st century hydroclimate of southwestern North America. *Proc. Natl. Acad. Sci. USA*, **107**, 21 277–21 282, https://doi.org/10.1073/pnas.0910856107.

——, M. Ting, C. Li, N. Naik, B. Cook, J. Nakamura, and H. Liu, 2013: Projections of declining surface-water availability for the southwestern United States. *Nat. Climate Change*, **3**, 482–486, https://doi.org/10.1038/nclimate1787.

Seth, A., S. A. Rauscher, M. Rojas, A. Giannini, and S. J. Camargo, 2011: Enhanced spring convective barrier for monsoons in a warmer world? *Climatic Change*, **104**, 403–414, https://doi.org/10.1007/s10584-010-9973-8.

Sharifi, E., J. Eitzinger, and W. Dorigo, 2019: Performance of the state-of-the-art gridded precipitation products over mountainous terrain: A regional study over Austria. *Remote Sens.*, **11**, 2018, https://doi.org/10.3390/rs11172018.

Singh, M. S., and P. A. O'Gorman, 2014: Influence of microphysics on the scaling of precipitation extremes with temperature. *Geophys. Res. Lett.*, **41**, 6037–6044, https://doi.org/10.1002/2014GL061222.

Stahle, D. W., and Coauthors, 2009: Cool- and warm-season precipitation reconstructions over western New Mexico. *J. Climate*, **22**, 3729–3750, https://doi.org/10.1175/2008JCLI2752.1.

Tabari, A., 2020: Climate change impact on flood and extreme precipitation increases with water availability. *Sci. Rep.*, **10**, 13768, https://doi.org/10.1038/s41598-020-70816-2.

Tippett, M. K., S. J. Camagro, and A. H. Sobel, 2011: A Poisson regression index for tropical cyclone genesis and the role of large-scale vorticity in genesis. *J. Climate*, **24**, 2335–2357, https://doi.org/10.1175/2010JCLI3811.1.

Torres-Alavez, A., T. Cavazos, and C. Turrent, 2014: Land–sea thermal contrast and intensity of the North American monsoon under climate change conditions. *J. Climate*, **27**, 4566–4580, https://doi.org/10.1175/JCLI-D-13-00557.1.

Xu, Z., Z. Wu, H. He, X. Wu, J. Zhou, Y. Zhang, and X. Guo, 2019: Evaluating the accuracy of MSWEP V2.1 and its performance for drought monitoring over mainland China. *Atmos. Res.*, **226**, 17–31, https://doi.org/10.1016/j.atmosres.2019.04.008.

Zhang, Y., T. Li, B. Wang, and G. Wu, 2002: Onset of the summer monsoon over the Indochina Peninsula: Climatology and interannual variations. *J. Climate*, **15**, 3206–3221, https://doi.org/10.1175/1520-0442(2002)015<3206:OOTSMO>2.0.CO;2.

Zhao, J., T. Y. Gan, G. Zhang, and S. Zhang, 2023: Projected changes of precipitation extremes in North America using CMIP6 multi-climate model ensembles. *J. Hydrol.*, **621**, 129598, https://doi.org/10.1016/j.jhydrol.2023.129598.